

Residue imaginary velocity induces many-body delocalization

Shi-Xin Hu, Yongxu Fu,* and Yi Zhang†

International Center for Quantum Materials, School of Physics, Peking University, Beijing, 100871, China

(Dated: July 24, 2024)

Localization and delocalization are historic topics central to quantum and condensed matter physics. We discover a new delocalization mechanism attributed to a residue imaginary (part of) velocity $\text{Im}(v)$, feasible for ground states or low-temperature states of non-Hermitian quantum systems under periodic boundary conditions. Interestingly, a disorder field contributing to $\text{Im}(v)$ may allow strong-disorder-limit delocalization when $\text{Im}(v)$ prevails over the Anderson localization. We demonstrate such delocalization with correlation and entanglement behaviors, as well as its many-body nature and generalizability to finite temperatures and interactions. Thus, the nontrivial physics of $\text{Im}(v)$ significantly enriches our understanding of delocalization and breeds useful applications, e.g., in quantum adiabatic processes.

Introduction— Commonly present due to mechanisms such as band insulators [1–11], interaction-driven Mott insulators [12–19], and disorder-induced Anderson insulators [20–26], localization is a crucial concept with vital consequences on physical properties like transport and spectrum [14–18, 22–33]. In general, the localization inevitably appears once the disorder strength reaches a threshold in disordered electronic systems, i.e., the Anderson transition from metallic to localized phases [26]. The dimensionality and symmetries play an essential role: the disorder is more relevant in lower dimensions, and an infinitesimal disorder in a one-dimensional (1D) Hermitian system leads to Anderson localization with all eigenstates and correlation functions necessarily localized [25].

Recent studies on effective non-Hermitian systems, including open quantum systems [34–41], optical systems (non-unitary quantum walk) [42–47], electric circuits [48–53], among others, have significantly broadened our understanding of condensed matter physics [54–57]. The non-Hermitian skin effect (NHSE), which supports an extensive number of single-particle eigenstates localized at the boundaries and characterized through the non-Bloch band theory with generalized Brillouin zones [58–60], reveals an additional localization formalism in 1D non-Hermitian systems under open-boundary conditions (OBCs) [58–62] and generalizable to higher dimensions [63–72]. With the introduction of disorder in non-Hermitian systems, e.g., the 1D Hatano-Nelson (HN) model [73], a mobility edge coinciding with the parity-time (PT) transition may emerge yet eventually give way to complete Anderson localization in the strong disorder limit [74–80]. Nonetheless, such Anderson localization and NHSE physics are mainly limited to a single-particle framework and represented by single-particle wave functions [81–89].

Here, we introduce a novel delocalization mechanism induced by a residue imaginary velocity $\text{Im}(v)$. While the velocity expectation values for ground states or low-temperature states $\hat{\rho} \propto \exp(-\beta\hat{H})$ generally possess a

vanishing real part [90], they may sustain a finite imaginary part $\text{Im}(v)$ in non-Hermitian quantum systems under periodic boundary conditions (PBCs). Such a residue $\text{Im}(v)$ mandates cumulative displacements in imaginary time, i.e., path integral, resulting in relevant world-lines traversing and winding around the system, as observed in quantum Monte Carlo stochastic series expansion (QMC-SSE) calculations [91]. Consequently, $\text{Im}(v)$ offers straightforward criteria for corresponding delocalization behaviors, including power-law correlation and quasi-long-range entanglement.

Interestingly, there are disorders that positively contribute to $\text{Im}(v)$ and may support delocalization even in the strong disorder limit when the $\text{Im}(v)$ physics prevails over their intrinsic Anderson localization, which was never possible before. Such delocalization also presents a many-body nature entirely distinctive from the previous mechanisms: the single-particle wave functions remain localized; nevertheless, the significant displacements between the Fermi sea’s left and right eigenstates establish global communications. Therefore, the physics of $\text{Im}(v)$, which is also straightforwardly generalizable to finite temperatures and interactions, greatly enriches our understanding of delocalization and bears potential applications - such as enhanced efficiency in quantum adiabatic process as we demonstrate in numerical examples.

Physics of the residue imaginary velocity— The expectation value of the velocity operator $\hat{v} = -i[x, \hat{H}]$ for the ground state or low-temperature density operator $\hat{\rho} \propto \exp(-\beta\hat{H})$ represents the macroscopic net velocity at equilibrium, which naturally vanishes for a Hermitian system \hat{H} . Non-Hermitian Hamiltonians, on the other hand, may effectively describe open or non-equilibrium (e.g., dissipative) quantum systems [92]. Consequently, the expectation value of \hat{v} may yield a nonzero net contribution for non-Hermitian quantum systems under PBCs and bring about interesting physics.

Let’s consider a translation-invariant system under PBC, e.g., the HN model:

$$\hat{H}_{\text{HN}} = \sum_x (1 + \delta)c_{x+1}^\dagger c_x + (1 - \delta)c_x^\dagger c_{x+1} = \sum_k \epsilon_k c_k^\dagger c_k, \quad (1)$$

where $\epsilon_k = 2 \cos k - 2i\delta \sin k$ is its PBC spectrum; see the

* yongxufu@pku.edu.cn

† frankzhangyi@gmail.com

deep-blue curve in Fig. 1(a). The velocity is summed over the Fermi Sea:

$$v = \sum_{\text{Re}(\epsilon_k) < \mu} v_k = \frac{L}{2\pi} (\epsilon_{k_{F,R}} - \epsilon_{k_{F,L}}), \quad (2)$$

where $v_k = \partial\epsilon_k/\partial k$, and $k_{F,R}$ ($k_{F,L}$) is the right (left) Fermi point [93]. For a Hermitian system, e.g., the HN model with $\delta = 0$, $\epsilon_k \in \mathbb{R}$, we have $\epsilon_{k_{F,R}} = \epsilon_{k_{F,L}} = \mu$, and $v = 0$. For a non-Hermitian system, on the other hand, $\epsilon_k \in \mathbb{C}$; while μ equalizes the Fermi energies' real parts $\text{Re}(\epsilon_{k_{F,R}}) = \text{Re}(\epsilon_{k_{F,L}}) = \mu$, their imaginary parts may differ $\text{Im}(\epsilon_{k_{F,R}}) \neq \text{Im}(\epsilon_{k_{F,L}})$, leading to a residue imaginary velocity $\text{Im}(v)$. Indeed, as μ varies, $\text{Im}(v)$ consistently follows the corresponding traverse in the complex spectrum; see Fig. 1(b). Here, we have focused on the ground state $\beta \rightarrow \infty$, but the arguments also apply to low-temperature scenarios, as we will discuss later.

Such a residue $\text{Im}(v)$ has far-reaching physical impacts. Semiclassically, its quantum dynamics characterize unidirectional displacements in imaginary time τ , i.e., relevant worldlines in (1+1)D path integral incline to shift cumulatively and circle the system [Fig. 1(c)]:

$$w_{opt} = \frac{dx}{d\tau} \cdot \frac{\beta}{L} = \text{Im}(v) \cdot \beta/L, \quad (3)$$

where w_{opt} is the winding number during an imaginary time of β , and L is the system size. Fig. 1(d) shows such nontrivial w_{opt} , obtained in QMC-SSE calculations of non-Hermitian quantum systems under PBCs [91], compares consistently with $\text{Im}(v)$. Importantly, such $\text{Im}(v) \neq 0$ mandates dominant path-integral trajectories traverse the entire system, causing delocalized physical behaviors, e.g., globalized correlation and entanglement, as we will show later [94]. We note that previous studies have also shown that states on the spectrum loops of non-Hermitian systems are more likely to delocalize [74, 77, 78]. Unlike previous delocalization formalisms with extended single-particle wave functions, however, we will show that the $\text{Im}(v)$ delocalization is essentially many-body in nature.

The physics of $\text{Im}(v)$ also applies to systems without translation symmetry, e.g., in the presence of disorder, where we can substitute the single-particle momentum k with the phase ϕ across the periodic boundary. We have included results of the HN models with random disorder $\hat{H}_{dis} = \sum_x \gamma_x c_x^\dagger c_x$, $\gamma_x \in [-\Gamma, \Gamma]$, in Fig. 1. The Anderson localization competes with $\text{Im}(v)$; as Γ increases and gradually overwhelms the $\text{Im}(v)$ delocalization, the complex spectrum loop shrinks, and accordingly, $\text{Im}(v)$'s amplitude and allowed μ window decreases [95], until $\Gamma \geq 4$ where the entire spectrum collapses into a line on the real axis and $\text{Im}(v)$ vanishes everywhere [96]. Consequently, $\text{Im}(v)$ offers a straightforward signature of systematic delocalization [97], as we will demonstrate with various examples later and in the supplemental materials. We emphasize that the residue $\text{Im}(v)$ is only present under PBCs, as both the velocity v and the path-integral wind-

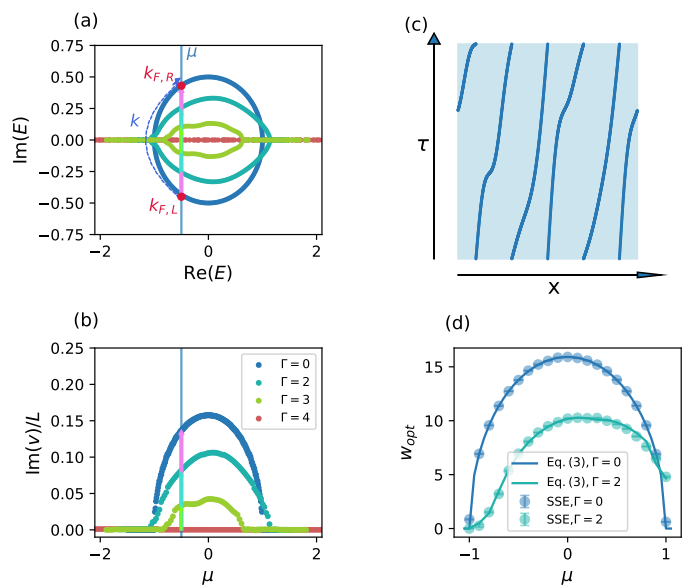


FIG. 1. (a) The complex spectra and (b) the imaginary (part of) velocity $\text{Im}(v)$ of the HN model under PBCs and different disorder strengths Γ show general correspondences. The vectors connecting Fermi points in the complex energy space (colored arrows) dictate the residue $\text{Im}(v)$ at that specific μ . The dashed arrow indicates the direction of increasing k for the pristine HN model with $\Gamma = 0$. (c) The path-integral trajectories in (1+1)D space-time may circle the system, e.g., winding number $w_{opt} = 1$, and (d) the dominant w_{opt} in QMC-SSE calculations ($\beta = 100$) compare consistently with $\text{Im}(v)$ and Eq. 3 for HN models. We set $\delta = 0.5$ and $L = 62$.

ing number w_{opt} are bound to vanish under open boundary conditions (OBCs), even if the rest of the settings are identical - in sharp contrast with previous delocalization generally insensitive to boundary conditions.

Delocalization behaviors and strong disorder limit—Inspired by the dissipative fluxed model in Ref. 98, we consider the 1D non-Hermitian Hamiltonian as follows:

$$\hat{H}_{AB} = \sum_x (a_{x+1}^\dagger a_x + b_x^\dagger a_x + a_{x+1}^\dagger b_x e^{i\phi(x)} + \text{h. c.}) + \gamma(x) b_x^\dagger b_x, \quad (4)$$

where a_x^\dagger (b_x^\dagger) is the fermion creation operator on the A (B) sublattice of site x , and $\gamma(x)$ ($\phi(x)$) is an onsite potential (flux); see illustration in Fig. 2(a). Fig. 2(b) shows its complex spectrum and residue imaginary velocity $\text{Im}(v)$ with translation-invariant $\gamma(x) = 3i$, $\phi(x) = \pi/2$ and PBC; as we invert either $\gamma(x)$ or $\phi(x)$, equivalent to a Hermitian or inversion transformation, respectively, $\text{Im}(v)$ changes sign. In comparison, real $\gamma(x)$ does not contribute to $\text{Im}(v)$, since Hermitian systems (real spectrum) always impose the vanishing of $\text{Im}(v)$. We discuss more general settings of Eq. 4 in the supplemental materials.

This motivates us to introduce the following correlated

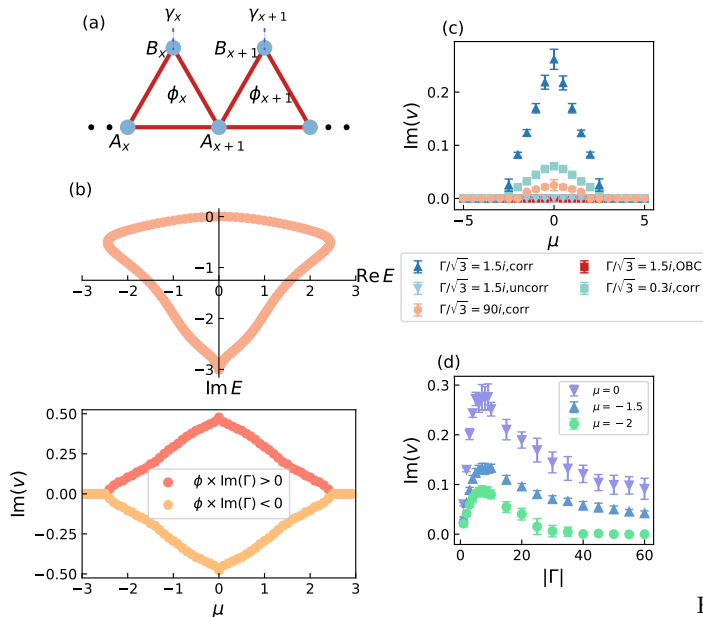


FIG. 2. (a) The model in Eq. (4) consists of an on-site potential $\gamma(x)$ on the B sublattice and a flux $\phi(x)$ on each lattice site x . (b) The complex spectrum and $\text{Im}(v)$ of a translation invariant model with $\gamma(x) = 3i$ and $\phi(x) = \pi/2$. $\text{Im}(v)$ changes sign as we flip $\gamma(x) = \pm 3i$ or $\phi(x) = \pm\pi/2$. (c) and (d): While $\text{Im}(v) \neq 0$ within a wide range of μ for various imaginary Γ and correlated phase $\phi(x)$ under PBCs, even strong disorder $|\Gamma| \gg 1$, it vanishes for real Γ , uncorrelated $\phi(x)$, or OBCs.

disorder $\gamma(x) = \Gamma U(x)$, $\Gamma/i \in \mathbb{R}$, $U(x) \in [-1, 1]$, and:

$$\phi(x) = \begin{cases} \pi/2, & U(x) > 0, \\ -\pi/2, & U(x) < 0, \end{cases} \quad (5)$$

so that despite of the randomness in $\gamma(x)$, the aligned signs between $\gamma(x)$ and $\phi(x)$ keep consistent contributions to $\text{Im}(v)$. Hence, such a disorder configuration evokes both the Anderson localization and $\text{Im}(v)$ delocalization. Indeed, unlike the uncorrelated disorder where $\gamma(x)$ and $\phi(x)$ are independent and $\text{Im}(v)$ vanishes, $\text{Im}(v)$ may remain finite if delocalization eventually prevails, e.g., μ near zero where the pristine model's spectrum spread thus $\gamma(x)$'s contribution to $\text{Im}(v)$ is largest; see Figs. 2(c) and 2(d) for a summary of the results. Notably, $\text{Im}(v)$ may remain finite only when we have imaginary $\gamma(x)$, correlated phase $\phi(x)$ as in Eq. 5, and PBCs.

Interestingly, we may obtain a fully delocalized system in the strong disorder limit for the first time. Our numerical results indeed suggest that despite peaking at intermediate $|\Gamma|$, $\text{Im}(v)$ survives even at very strong disorder $|\Gamma| \gg 1$ [Fig. 2(d)]; see a semi-quantitative discussion of the strong disorder limit in the supplemental materials.

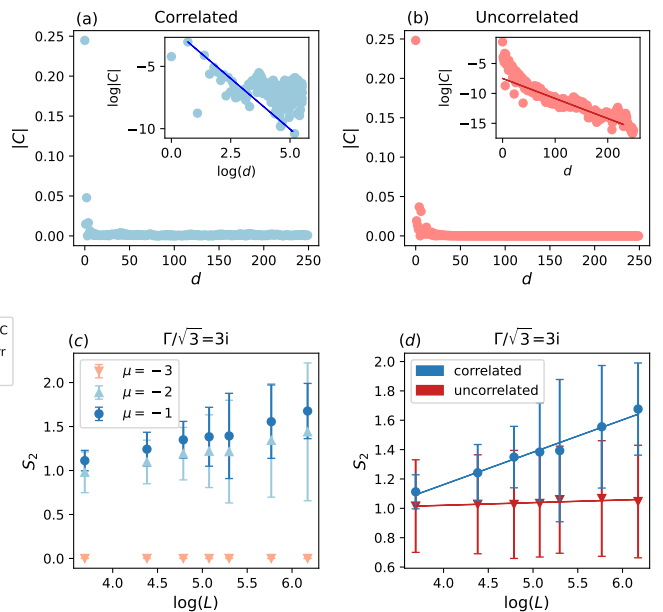


FIG. 3. The correlation functions between the A sublattices of the model in Eq. 4 exhibit (a) a power-law scaling for phase-correlated disorder (Eq. 5) and (b) an exponential decay for uncorrelated disorder. We set $\Gamma = 1.5 \times \sqrt{3}i$, $\mu = -1$, and the system size $L = 1000$. The insets are log-log and log-linear plots, respectively. Likewise, the second Renyi entropy S_2 shows an area law for the localized scenarios [$\mu = -3$ case in (c) and uncorrelated case in (d)] and a logarithmic correction, i.e., $S_2 \propto \log(L)$, for the delocalized scenarios [$\mu = -1, -2$ cases in (c) and the phase-correlated case in (d)]. We implement phase-correlated disorder in (c) and $\mu = -1$ in (d).

Such a delocalized behavior is in sheer contrast with the disordered HN models, where the only role disorder plays is the Anderson localization, which eventually suppresses whatever non-disorder-based delocalization in the strong disorder limit [74–80].

The delocalization exhibits clear physical signatures in correlation and entanglement: the correlation functions $C(d) = \frac{1}{N} \sum_x \langle c_x^\dagger c_{x+d} \rangle$ exhibit a power-law scaling with respect to spatial distance d in the delocalized case where $\text{Im}(v)$ remains finite [Fig. 3(a)] yet an exponential decay in the localized case where $\text{Im}(v)$ vanishes [Fig. 3(b)]; the second Renyi entropy $S_2 = -\log \text{tr}(\hat{\rho}^2)$ also exhibit quasi-long-range behaviors with logarithmic corrections $S_2 \propto \log(L)$ [$\mu = -1$ and $\mu = -2$ in Fig. 3(c), correlated case in Fig. 3(d)] in scenarios that coincide with a finite $\text{Im}(v)$, instead of the Area-Law behaviors otherwise [$\mu = -3$ in Fig. 3(c), uncorrelated case in Fig. 3(d)]. Here, $\hat{\rho}$ is the reduced density operator on half of the system [91]. Compared with $C(d)$ or S_2 , v concerns mostly local operators and is thus much more straightforward to evaluate for (de)localization identifications.

Many-body delocalization— Commonly, a defining signature accompanying delocalization is the extended wave functions. However, this is no longer true for the $\text{Im}(v)$ delocalization in strong disorder. Despite overall (quasi-

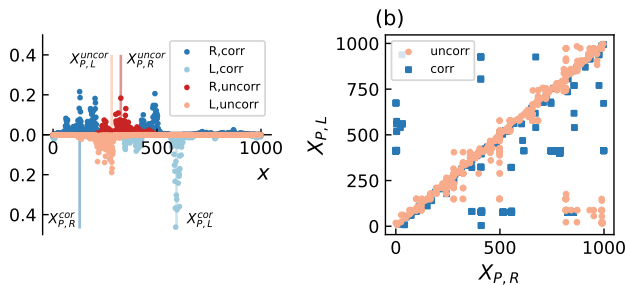


FIG. 4. (a) Typical distributions of a pair of left and right eigenstates of non-Hermitian systems in Eq. 4 with $\Gamma = 5i$ and either correlated or uncorrelated phase $\phi(x)$ show localized single-particle wave functions. We mark their peak locations as $X_{P,R}$ and $X_{P,L}$, respectively. (b) However, while the distributions of left and right eigenstates closely shadow each other in the former scenario, they may differ significantly and globally in the presence of a residue $\text{Im}(v)$, as we illustrate with correspondence between the peak locations $X_{P,R}$ and $X_{P,L}$ for various pair of states. Note that $X_{P,R} \sim X_{P,L}$ at the top left and bottom right corners due to PBCs.

long-range correlation and entanglement of disordered \hat{H}_{AB} , its single-particle left eigenstates $|\psi_n^L\rangle$ and right eigenstates $|\psi_n^R\rangle$ still behave localized; see Fig. 4(a) for examples. Previous works have also found that once strong disorder's Anderson localization dominates over the NHSE under OBCs, non-Hermitian systems' single-particle states become exponentially localized in real space around respective sites [75–83].

Instead, the $\text{Im}(v)$ delocalization is essentially a quantum many-body effect, taking a vastly different origin: when $\text{Im}(v)$ vanishes and localization looms, a pair of $|\psi_n^R\rangle$ and $|\psi_n^L\rangle$ closely shadow each other's real-space distributions and differ only locally; this resembles Hermitian quantum systems where $|\psi_n^R\rangle$ and $|\psi_n^L\rangle$ are conjugates with identical distributions [99]; in contrast, however, when $\text{Im}(v) \neq 0$ and many-body delocalization occurs, $|\psi_n^R\rangle$ and $|\psi_n^L\rangle$, though respectively localized, may concentrate at vastly different and globally distant regions, as are apparent from their respective peak positions $X_{P,R}$ and $X_{P,L}$ in Fig. 4. Consequently, the quantum many-body density operator $\hat{\rho} \propto \exp(-\beta\hat{H})$ establishes remote communication through $|\psi_n^L\rangle\langle\psi_n^R|$, summed over the Fermi Sea, which is present in many-body properties such as path-integral worldlines, correlation, and entanglement. In short, despite the non-interacting systems examples, the $\text{Im}(v)$ delocalization has nothing to do with delocalized single-particle wave functions [100].

Such many-body nature also suggests straightforward generalizations to finite temperature and interaction. At finite $\beta = 1/k_B T$, $\exp(-\beta\hat{H}) = \sum_n f(\epsilon_n) |nR\rangle\langle nL|$, where $f(\epsilon_n) = 1/(\exp^{\beta\epsilon_n} + 1)$ tends to 1 (0) for $\text{Re}(\epsilon_n) \ll k_B T$ ($\text{Re}(\epsilon_n) \gg -k_B T$), filling the Fermi Sea; only states within the energy window $|\text{Re}(\epsilon_n)| \lesssim k_B T$ make complex contributions and cause deviations, which are small at large β . A systematic delocalization emerges if a residue

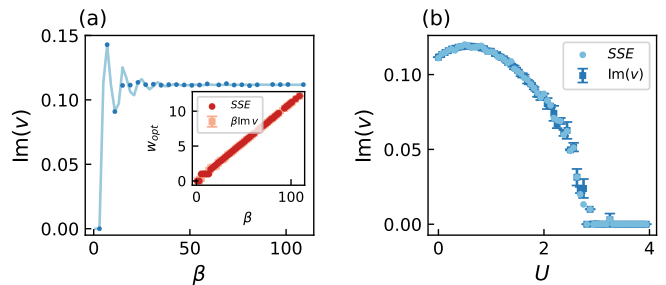


FIG. 5. (a) The residue imaginary velocity $\text{Im}(v)$ of the HN model \hat{H}_{HN} initiates from 0 at small β (high temperature) and eventually converges to a typical value at large β (low temperature). (b) The repulsive interaction U suppresses the delocalization and fully eliminates the residue $\text{Im}(v)$ at $U > 3$. $\text{Im}(v)$ trends consistently with the winding number w_{opt} of path-integral worldlines in both scenarios. $\delta = 0.5$ and $\mu = 0$.

$\text{Im}(v)$ remains. On the contrary, at high temperatures and small β , the path-integral worldlines may not possess sufficient imaginary time β to get across the system; thus, the $\text{Im}(v)$ delocalization should be impaired. Indeed, the results of $\text{Im}(v)$ for the HN model at various β in Fig. 5(a) verify our expectations. We also consider the HN model with the interaction $\hat{H}_U = U \sum_x \hat{n}_x \hat{n}_{x+1}$, where $\hat{n}_x = c_x^\dagger c_x$. A repulsive interaction $U > 0$ competes with and suppresses $\text{Im}(v)$ and gradually drives the system toward localization in a Mott-insulating fashion, as is summarized in Fig. 5(b).

Conclusions and discussions— We have discussed a new many-body delocalization mechanism attributed to a residue imaginary velocity $\text{Im}(v)$ for non-Hermitian quantum systems under PBCs. We demonstrated its presence in various models, including finite-temperature and interacting scenarios, and showed its nontrivial correlation and entanglement. Such $\text{Im}(v)$ delocalization may prevail over the Anderson localization and allow strong-disorder-limit delocalization, even when the corresponding single-particle states are fully localized. Thus, the nontrivial physics of $\text{Im}(v)$ significantly enriches our understanding of delocalization.

The $\text{Im}(v)$ delocalization may support interesting applications, e.g., quantum simulations and optimizations. For instance, a quantum adiabatic process obtains the ground state of a target Hamiltonian \hat{H}_1 by initializing a ground state at another \hat{H}_0 and interpolating $\hat{H}_\lambda = \lambda\hat{H}_1 + (1-\lambda)\hat{H}_0$, $\lambda \in [0, 1]$. In practice, however, such formalism breaks down when ground states change abruptly, commonly because they are localized at different, globally separated minimums. A residue $\text{Im}(v)$ enforces delocalization so that the many-body ground states may evolve more smoothly.

For example, we interpolate two disordered models in Eq. 4 under PBCs and evaluate the fidelity between ground states along the path. In particular, we consider cases with fully real $\gamma(x)$, as well as $\gamma(x)$ with imaginary components without and with correlated phase $\phi(x)$; see

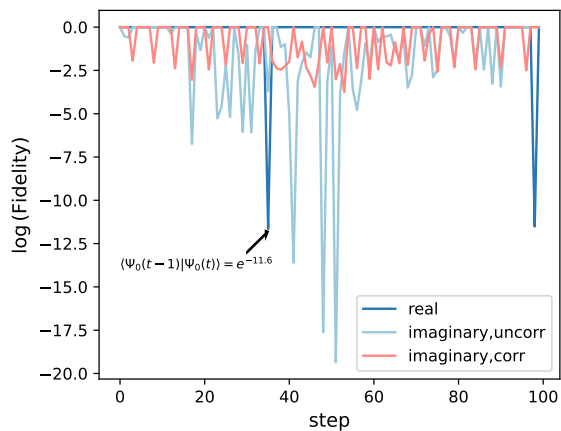


FIG. 6. The fidelity along interpolating paths between disordered Hamiltonians indicates significantly better adiabaticity, i.e., fidelity minima, in the presence of $\text{Im}(v)$ delocalization: unlike the localized cases [uncorrelated phase $\phi(x)$ or real-valued $\gamma(x)$] where the ground states suffer abrupt changes at isolated instances, the delocalized case is able to distribute the ground states' evolution more evenly along the path.

more detailed settings in supplemental materials. As we summarize in Fig. 6, when and only when we successfully establish a residue $\text{Im}(v)$, i.e., the latter scenario, the ground states evolve relatively smoothly and distribute their destined transformation more even along the process, while the other cases both witness collapsed fidelity thus abrupt changes to the ground states at one point or another. Importantly, such an advantage is only present under PBCs but not OBCs.

Acknowledgment: We acknowledge generous support from the National Key R&D Program of China (No.2022YFA1403700) and the National Natural Science Foundation of China (No.12174008 & No.92270102).

-
- [1] D. J. Thouless, M. Kohmoto, M. P. Nightingale, and M. den Nijs, Quantized hall conductance in a two-dimensional periodic potential, *Phys. Rev. Lett.* **49**, 405 (1982).
 - [2] F. D. M. Haldane, Model for a quantum hall effect without landau levels: Condensed-matter realization of the "parity anomaly", *Phys. Rev. Lett.* **61**, 2015 (1988).
 - [3] C. L. Kane and E. J. Mele, Z_2 topological order and the quantum spin hall effect, *Phys. Rev. Lett.* **95**, 146802 (2005).
 - [4] C. L. Kane and E. J. Mele, Quantum spin hall effect in graphene, *Phys. Rev. Lett.* **95**, 226801 (2005).
 - [5] B. A. Bernevig, T. L. Hughes, and S.-C. Zhang, Quantum spin hall effect and topological phase transition in hgte quantum wells, *Science* **314**, 1757 (2006).
 - [6] L. Fu, C. L. Kane, and E. J. Mele, Topological insulators in three dimensions, *Phys. Rev. Lett.* **98**, 106803 (2007).
 - [7] A. H. Castro Neto, F. Guinea, N. M. R. Peres, K. S. Novoselov, and A. K. Geim, The electronic properties of graphene, *Rev. Mod. Phys.* **81**, 109 (2009).
 - [8] A. Kitaev, Periodic table for topological insulators and superconductors, *AIP Conference Proceedings* **1134**, 22 (2009).
 - [9] M. Z. Hasan and C. L. Kane, Colloquium: Topological insulators, *Rev. Mod. Phys.* **82**, 3045 (2010).
 - [10] X.-L. Qi and S.-C. Zhang, Topological insulators and superconductors, *Rev. Mod. Phys.* **83**, 1057 (2011).
 - [11] C.-K. Chiu, J. C. Y. Teo, A. P. Schnyder, and S. Ryu, Classification of topological quantum matter with symmetries, *Rev. Mod. Phys.* **88**, 035005 (2016).
 - [12] N. F. Mott and R. Peierls, Discussion of the paper by de boer and verwey, *Proceedings of the Physical Society* **49**, 72 (1937).
 - [13] N. F. Mott, The basis of the electron theory of metals, with special reference to the transition metals, *Proceedings of the Physical Society. Section A* **62**, 416 (1949).
 - [14] N. F. MOTT, Metal-insulator transition, *Rev. Mod. Phys.* **40**, 677 (1968).
 - [15] M. Imada, A. Fujimori, and Y. Tokura, Metal-insulator transitions, *Rev. Mod. Phys.* **70**, 1039 (1998).
 - [16] P. Fazekas, *Lecture Notes on Electron Correlation and Magnetism* (World Scientific, Singapore, 1999).
 - [17] P. A. Lee, N. Nagaosa, and X.-G. Wen, Doping a mott insulator: Physics of high-temperature superconductivity, *Rev. Mod. Phys.* **78**, 17 (2006).
 - [18] S. B. Roy, Mott insulators and related phenomena: a basic introduction, in *Mott Insulators*, 2053-2563 (IOP Publishing, 2019) pp. 3-1 to 3-35.
 - [19] H. Pan and S. Das Sarma, Interaction-driven filling-induced metal-insulator transitions in 2d moiré lattices, *Phys. Rev. Lett.* **127**, 096802 (2021).
 - [20] P. W. Anderson, Absence of diffusion in certain random lattices, *Phys. Rev.* **109**, 1492 (1958).
 - [21] E. Abrahams, P. W. Anderson, D. C. Licciardello, and T. V. Ramakrishnan, Scaling theory of localization: Absence of quantum diffusion in two dimensions, *Phys. Rev. Lett.* **42**, 673 (1979).
 - [22] A. MacKinnon and B. Kramer, The scaling theory of electrons in disordered solids: Additional numerical results, *Zeitschrift für Physik B Condensed Matter* **53**, 1 (1983).
 - [23] P. A. Lee and T. V. Ramakrishnan, Disordered electronic systems, *Rev. Mod. Phys.* **57**, 287 (1985).
 - [24] B. Kramer and A. MacKinnon, Localization: theory and experiment, *Reports on Progress in Physics* **56**, 1469 (1993).
 - [25] P. W. Brouwer, P. G. Silvestrov, and C. W. J. Beenakker, Theory of directed localization in one dimension, *Phys. Rev. B* **56**, R4333 (1997).
 - [26] F. Evers and A. D. Mirlin, Anderson transitions, *Rev.*

- Mod. Phys. **80**, 1355 (2008).
- [27] K. v. Klitzing, G. Dorda, and M. Pepper, New method for high-accuracy determination of the fine-structure constant based on quantized hall resistance, Phys. Rev. Lett. **45**, 494 (1980).
- [28] R. B. Laughlin, Quantized hall conductivity in two dimensions, Phys. Rev. B **23**, 5632 (1981).
- [29] D. J. Thouless, Quantization of particle transport, Phys. Rev. B **27**, 6083 (1983).
- [30] Q. Niu and D. J. Thouless, Quantised adiabatic charge transport in the presence of substrate disorder and many-body interaction, Journal of Physics A: Mathematical and General **17**, 2453 (1984).
- [31] Q. Niu, D. J. Thouless, and Y.-S. Wu, Quantized hall conductance as a topological invariant, Phys. Rev. B **31**, 3372 (1985).
- [32] Y. Hatsugai, Chern number and edge states in the integer quantum hall effect, Phys. Rev. Lett. **71**, 3697 (1993).
- [33] Y. Hatsugai, Edge states in the integer quantum hall effect and the riemann surface of the bloch function, Phys. Rev. B **48**, 11851 (1993).
- [34] I. Rotter, A non-hermitian hamilton operator and the physics of open quantum systems, Journal of Physics A: Mathematical and Theoretical **42**, 153001 (2009).
- [35] S. Malzard, C. Poli, and H. Schomerus, Topologically protected defect states in open photonic systems with non-hermitian charge-conjugation and parity-time symmetry, Phys. Rev. Lett. **115**, 200402 (2015).
- [36] H. J. Carmichael, Quantum trajectory theory for cascaded open systems, Phys. Rev. Lett. **70**, 2273 (1993).
- [37] C. Guo and D. Poletti, Solutions for bosonic and fermionic dissipative quadratic open systems, Phys. Rev. A **95**, 052107 (2017).
- [38] F. Dangel, M. Wagner, H. Cartarius, J. Main, and G. Wunner, Topological invariants in dissipative extensions of the su-schrieffer-heeger model, Phys. Rev. A **98**, 013628 (2018).
- [39] F. Song, S. Yao, and Z. Wang, Non-hermitian skin effect and chiral damping in open quantum systems, Phys. Rev. Lett. **123**, 170401 (2019).
- [40] A. McDonald, R. Hanai, and A. A. Clerk, Nonequilibrium stationary states of quantum non-hermitian lattice models, Phys. Rev. B **105**, 064302 (2022).
- [41] A. Altland, M. Fleischhauer, and S. Diehl, Symmetry classes of open fermionic quantum matter, Phys. Rev. X **11**, 021037 (2021).
- [42] A. Guo, G. J. Salamo, D. Duchesne, R. Morandotti, M. Volatier-Ravat, V. Aimez, G. A. Siviloglou, and D. N. Christodoulides, Observation of \mathcal{PT} -symmetry breaking in complex optical potentials, Phys. Rev. Lett. **103**, 093902 (2009).
- [43] W. Chen, Ş. Kaya Özdemir, G. Zhao, J. Wiersig, and L. Yang, Exceptional points enhance sensing in an optical microcavity, Nature **548**, 192 (2017).
- [44] L. Xiao, K. Wang, X. Zhan, Z. Bian, K. Kawabata, M. Ueda, W. Yi, and P. Xue, Observation of critical phenomena in parity-time-symmetric quantum dynamics, Phys. Rev. Lett. **123**, 230401 (2019).
- [45] L. Xiao, T. Deng, K. Wang, G. Zhu, Z. Wang, W. Yi, and P. Xue, Non-hermitian bulk-boundary correspondence in quantum dynamics, Nature Physics **16**, 761 (2020).
- [46] L. Xiao, T. Deng, K. Wang, Z. Wang, W. Yi, and P. Xue, Observation of non-bloch parity-time symmetry and exceptional points, Phys. Rev. Lett. **126**, 230402 (2021).
- [47] L. Xiao, W.-T. Xue, F. Song, Y.-M. Hu, W. Yi, Z. Wang, and P. Xue, Observation of non-hermitian edge burst in quantum dynamics (2023), arXiv:2303.12831 [cond-mat.mes-hall].
- [48] M. Ezawa, Non-hermitian boundary and interface states in nonreciprocal higher-order topological metals and electrical circuits, Phys. Rev. B **99**, 121411 (2019).
- [49] M. Ezawa, Electric circuits for non-hermitian chern insulators, Phys. Rev. B **100**, 081401 (2019).
- [50] T. Hofmann, T. Helbig, F. Schindler, N. Salgo, M. Brzezińska, M. Greiter, T. Kiessling, D. Wolf, A. Vollhardt, A. Kabaš, C. H. Lee, A. Bilušić, R. Thomale, and T. Neupert, Reciprocal skin effect and its realization in a topoelectrical circuit, Phys. Rev. Res. **2**, 023265 (2020).
- [51] T. Helbig, T. Hofmann, S. Imhof, M. Abdelghany, T. Kiessling, L. W. Molenkamp, C. H. Lee, A. Szameit, M. Greiter, and R. Thomale, Generalized bulk-boundary correspondence in non-hermitian topoelectrical circuits, Nature Physics **16**, 747 (2020).
- [52] L. Li, C. H. Lee, and J. Gong, Impurity induced scale-free localization, Communications Physics **4**, 42 (2021).
- [53] H. Hu and E. Zhao, Knots and non-hermitian bloch bands, Phys. Rev. Lett. **126**, 010401 (2021).
- [54] E. J. Bergholtz, J. C. Budich, and F. K. Kunst, Exceptional topology of non-hermitian systems, Rev. Mod. Phys. **93**, 015005 (2021).
- [55] A. Yuto, G. Zongping, and U. Masahito, Non-hermitian physics, Advances in Physics **69**, 249 (2020).
- [56] Z. Gong, Y. Ashida, K. Kawabata, K. Takasan, S. Higashikawa, and M. Ueda, Topological phases of non-hermitian systems, Phys. Rev. X **8**, 031079 (2018).
- [57] K. Kawabata, K. Shiozaki, M. Ueda, and M. Sato, Symmetry and topology in non-hermitian physics, Phys. Rev. X **9**, 041015 (2019).
- [58] S. Yao and Z. Wang, Edge states and topological invariants of non-hermitian systems, Phys. Rev. Lett. **121**, 086803 (2018).
- [59] K. Yokomizo and S. Murakami, Non-bloch band theory of non-hermitian systems, Phys. Rev. Lett. **123**, 066404 (2019).
- [60] Z. Yang, K. Zhang, C. Fang, and J. Hu, Non-hermitian bulk-boundary correspondence and auxiliary generalized brillouin zone theory, Phys. Rev. Lett. **125**, 226402 (2020).
- [61] K. Zhang, Z. Yang, and C. Fang, Correspondence between winding numbers and skin modes in non-hermitian systems, Phys. Rev. Lett. **125**, 126402 (2020).
- [62] N. Okuma, K. Kawabata, K. Shiozaki, and M. Sato, Topological origin of non-hermitian skin effects, Phys. Rev. Lett. **124**, 086801 (2020).
- [63] T. Liu, Y.-R. Zhang, Q. Ai, Z. Gong, K. Kawabata, M. Ueda, and F. Nori, Second-order topological phases in non-hermitian systems, Phys. Rev. Lett. **122**, 076801 (2019).
- [64] C. H. Lee, L. Li, and J. Gong, Hybrid higher-order skin-topological modes in nonreciprocal systems, Phys. Rev. Lett. **123**, 016805 (2019).
- [65] R. Okugawa, R. Takahashi, and K. Yokomizo, Second-order topological non-hermitian skin effects, Phys. Rev.

- B **102**, 241202 (2020).
- [66] K. Kawabata, M. Sato, and K. Shiozaki, Higher-order non-hermitian skin effect, *Phys. Rev. B* **102**, 205118 (2020).
- [67] Y. Fu, J. Hu, and S. Wan, Non-hermitian second-order skin and topological modes, *Phys. Rev. B* **103**, 045420 (2021).
- [68] Y. Li, C. Liang, C. Wang, C. Lu, and Y.-C. Liu, Gain-loss-induced hybrid skin-topological effect, *Phys. Rev. Lett.* **128**, 223903 (2022).
- [69] K. Yokomizo and S. Murakami, Non-bloch bands in two-dimensional non-hermitian systems, *Phys. Rev. B* **107**, 195112 (2023).
- [70] H.-Y. Wang, F. Song, and Z. Wang, Amoeba formulation of non-bloch band theory in arbitrary dimensions, *Phys. Rev. X* **14**, 021011 (2024).
- [71] H. Hu, Non-hermitian band theory in all dimensions: uniform spectra and skin effect (2023), arXiv:2306.12022 [cond-mat.mes-hall].
- [72] Y. Xiong, Z.-Y. Xing, and H. Hu, Non-hermitian skin effect in arbitrary dimensions: non-bloch band theory and classification (2024), arXiv:2407.01296 [cond-mat.mes-hall].
- [73] N. Hatano and D. R. Nelson, Localization transitions in non-hermitian quantum mechanics, *Phys. Rev. Lett.* **77**, 570 (1996).
- [74] S. Longhi, Topological phase transition in non-hermitian quasicrystals, *Phys. Rev. Lett.* **122**, 237601 (2019).
- [75] H. Jiang, L.-J. Lang, C. Yang, S.-L. Zhu, and S. Chen, Interplay of non-hermitian skin effects and anderson localization in nonreciprocal quasiperiodic lattices, *Phys. Rev. B* **100**, 054301 (2019).
- [76] S. Longhi, Metal-insulator phase transition in a non-hermitian aubry-andré-harper model, *Phys. Rev. B* **100**, 125157 (2019).
- [77] T. Liu, H. Guo, Y. Pu, and S. Longhi, Generalized aubry-andré self-duality and mobility edges in non-hermitian quasiperiodic lattices, *Phys. Rev. B* **102**, 024205 (2020).
- [78] Y. Liu, X.-P. Jiang, J. Cao, and S. Chen, Non-hermitian mobility edges in one-dimensional quasicrystals with parity-time symmetry, *Phys. Rev. B* **101**, 174205 (2020).
- [79] Y. Liu, Q. Zhou, and S. Chen, Localization transition, spectrum structure, and winding numbers for one-dimensional non-hermitian quasicrystals, *Phys. Rev. B* **104**, 024201 (2021).
- [80] C. Yuce and H. Ramezani, Coexistence of extended and localized states in the one-dimensional non-hermitian anderson model, *Phys. Rev. B* **106**, 024202 (2022).
- [81] Q.-B. Zeng, Y.-B. Yang, and Y. Xu, Topological phases in non-hermitian aubry-andré-harper models, *Phys. Rev. B* **101**, 020201 (2020).
- [82] S. Longhi, Phase transitions in a non-hermitian aubry-andré-harper model, *Phys. Rev. B* **103**, 054203 (2021).
- [83] S. Longhi, Spectral deformations in non-hermitian lattices with disorder and skin effect: A solvable model, *Phys. Rev. B* **103**, 144202 (2021).
- [84] J. Claes and T. L. Hughes, Skin effect and winding number in disordered non-hermitian systems, *Phys. Rev. B* **103**, L140201 (2021).
- [85] N. Okuma and M. Sato, Non-hermitian skin effects in hermitian correlated or disordered systems: Quantities sensitive or insensitive to boundary effects and pseudo-quantum-number, *Phys. Rev. Lett.* **126**, 176601 (2021).
- [86] R. Sarkar, S. S. Hegde, and A. Narayan, Interplay of disorder and point-gap topology: Chiral modes, localization, and non-hermitian anderson skin effect in one dimension, *Phys. Rev. B* **106**, 014207 (2022).
- [87] Q. Lin, T. Li, L. Xiao, K. Wang, W. Yi, and P. Xue, Observation of non-hermitian topological anderson insulator in quantum dynamics, *Nature Communications* **13**, 3229 (2022).
- [88] T. Orito and K.-I. Imura, Unusual wave-packet spreading and entanglement dynamics in non-hermitian disordered many-body systems, *Phys. Rev. B* **105**, 024303 (2022).
- [89] E. T. Kokkinakis, K. G. Makris, and E. N. Economou, Anderson localization versus hopping asymmetry in a disordered lattice (2024), arXiv:2407.10746 [cond-mat.dis-nn].
- [90] There may be further complexity due to either a complex μ or a complex phase factor $e^{i\theta} \hat{H}$ upon the Hamiltonian, which can be simplified via a rotation of the complex energy plane.
- [91] S.-X. Hu, Y. Fu, and Y. Zhang, Nontrivial worldline winding in non-hermitian quantum systems, *Phys. Rev. B* **108**, 245114 (2023).
- [92] Admittedly, the microscopic mechanism that an open or non-equilibrium system may induce a residue $\text{Im}(v)$ for a non-Hermitian Hamiltonian's thermal density operator $\hat{\rho} \propto \exp(-\beta \hat{H})$ remains an open question for future research.
- [93] Multiple bands or Fermi Seas also need to be summed over in case of their existence.
- [94] A residue $\text{Im}(v)$ under PBC may also be related to NHSE at the corresponding open boundary.
- [95] Similarly to Hermitian quantum systems, the localization begins at the band edges and moves toward the center.
- [96] We will systematically study the impacts of localization and boundary conditions on the non-Hermitian spectra in a separate work.
- [97] Unlike correlation and entanglement, $\text{Im}(v)$ mostly concerns more local operators that are simpler to evaluate.
- [98] Q. Liang, D. Xie, Z. Dong, H. Li, H. Li, B. Gadway, W. Yi, and B. Yan, Dynamic signatures of non-hermitian skin effect and topology in ultracold atoms, *Phys. Rev. Lett.* **129**, 070401 (2022).
- [99] $\text{Im}(v) = 0$ in Hermitian quantum systems thus the $\text{Im}(v)$ delocalization hardly materializes there.
- [100] On the contrary, localization requires both localized single-particle states and $\text{Im}(v) = 0$.